



Experimental performance comparison of shell-and-tube oil coolers with overlapped helical baffles and segmental baffles



Jian-Fei Zhang, Shao-Long Guo, Zhong-Zhen Li, Jin-Ping Wang, Ya-Ling He, Wen-Quan Tao*

Key Laboratory of Thermo-Fluid Science and Engineering, Ministry of Education, School of Power and Energy Engineering, Xi'an Jiaotong University, Xi'an 710049, China

HIGHLIGHTS

- The performance of OCHB and OCSB with practical size is experimentally investigated.
- The shell side heat transfer coefficients of the OCHB are lower than that of the OCSB.
- The shell-side pressure drop of the OCHB is far lower than that of the OCSB.
- The OCHB obtains higher heat transfer coefficient per unit pressure drop.
- With proper design OCHB can obtain better heat transfer performance.

ARTICLE INFO

Article history:

Received 20 December 2012

Accepted 8 April 2013

Available online 28 April 2013

Keywords:

Oil cooler

Helical baffle

Segmental baffle

Pressure drop

Heat transfer

ABSTRACT

Many research studies have been conducted on the performance of shell and tube heat exchanger with helical baffles because of its lower shell-side pressure drop, lower fouling resistance and lower operation and maintenance cost. But the extension of those studies into practical application is limited because of the additional effects caused by the small-size model. In this paper, the performance of shell-and-tube oil coolers with overlapped helical baffles and segmental baffles is compared experimentally, and both of the oil coolers are practical products. The results show that the OCHB (Oil Cooler with Helical Baffles) gets lower shell side pressure drop and higher heat transfer coefficient per unit pressure drop at fixed volume flow rate than the OCSB (Oil Cooler with Segmental Baffles). Based on the experimental data, it can be predicted that with proper design the OCHB can get better heat transfer performance than OCSB. The present studies are beneficial for the design and practical operation of OCSB and OCHB.

© 2013 Elsevier Ltd. All rights reserved.

1. Introduction

More than 35–40% of heat exchangers used in industrial areas are of the shell-and-tube heat exchangers (STHXs) due to their robust geometry construction, easy maintenance and possible upgrades [1]. The shell and tube oil cooler is widely used in the chemical engineering process and machining process, which maintains an oil (e.g. lubricating oil, conductive oil) supply at a consistent, optimal temperature. In STHXs, the shape and arrangement of baffles are of essential importance for the performance of heat exchangers. The most commonly used baffle is the segmental baffle, which forces the shell-side fluid to go through in a zigzag manner. But there are three major drawbacks in the

conventional shell-and-tube heat exchangers with segmental baffles (STHXsSB): (1) it causes a large shell-side pressure drop; (2) it results in a dead zone in each compartment between two adjacent segmental baffles, leading to an increase of fouling resistance; (3) the dramatic zigzag flow pattern also causes high risk of vibration failure on tube bundle.

To overcome the above-mentioned drawbacks of the conventional segmental baffle, a number of improvements were proposed to obtain higher heat transfer coefficient, lower possibility of tube vibration, and reduced fouling factor [2–7]. But the principal shortcomings of the conventional segmental baffle still remain. In the 1990s, a new type of baffle called helical baffle was first proposed by Lutcha and Nencansky [8] and then further studied by Stehlik et al. [9] and Kral et al. [10]. For the convenience of manufacturing, most helical baffles actually used in STHXs are noncontinuous approximate helicoids. The noncontinuous helical baffles are usually made by four elliptical sector-shaped plates, as

* Corresponding author.

E-mail address: wqtao@mail.xjtu.edu.cn (W.-Q. Tao).

shown in Fig. 1, where the helix angle, designated by β , helical pitch, B , and baffle thickness, S_p , are presented. Each baffle occupies one-quarter of the cross section of the heat exchanger and is angled to the axis of the heat exchanger. The two adjacent baffles may be joined end to end at the perimeter of each sector, forming a continuous helix at the outer periphery (Fig. 2). Another connection between two adjacent sectors is the overlapped connection, usually middle-overlapped as shown in Fig. 1. For heat exchangers with large shell diameters, the overlapped structures can reduce the helical pitch to shorten the length of heat exchanger and can also reduce the cross-flow area to obtain higher shell-side velocity. Therefore such connection is more popular in engineering practice. The OCHB tested in this paper is of this type (but not middle overlapped).

Many research studies have been done on the shell-and-tube heat exchangers with helical baffles (STHXsHB). Typical experiment studies of this subject since the year of 2000 are listed in Refs. [11–16]. Typical progresses in simulations of STHXsHB can be found in Refs. [17–25]. It should be noted that the rapid development of CFD commercial code and computer hardware helps the direct 3D numerical simulation of complex flow phenomenon in STHXsHB and it is becoming more and more convenient and popular.

Apart from the above studies, further improvement on the structure of shell and tube heat exchanger with non-continuous helical baffles has been proposed to overcome the shortcut flow in the shell side of shell-and-tube heat exchangers with non-continuous helical baffles. Wang and his co-workers proposed shell-and-tube heat exchangers with continuous helical baffles, shell-and-tube heat exchangers with combined helical baffles and combined multiple shell-pass shell-and-tube heat exchangers with continuous helical baffles [26–33]. Ji et al. [34] invented a double shell-pass shell-and-tube heat exchanger with continuous helical baffles (STHXCH) to improve the shell-side performance of STHXCH. Chen et al. [35] proposed a novel helical heat exchanger structure consisting of circumferential-overlap trisection helical baffle and numerically investigated the flow and heat transfer characteristic of the heat exchanger.

The geometries of STHXsHB being tested in above-mentioned experimental studies are listed in Table 1. From Table 1 it could be found that the most of the heat exchangers in those studies are small-size models and the sizes of most of the heat exchangers are smaller than $200 \text{ mm} \times 1000 \text{ mm}$ (Inner diameter of the shell \times Effective length). The spread of test results obtained in those studies in the design and operation of practical products might be limited due to the additional effects caused by models. In this paper, the performance of shell-and-tube oil coolers with overlapped helical baffles and segmental baffles is compared experimentally.

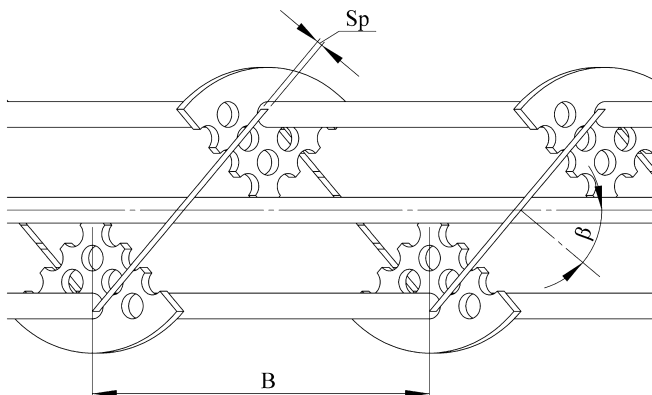


Fig. 1. Schematics of four pieces middle-overlapped helical baffle arrangement and parameters definition.

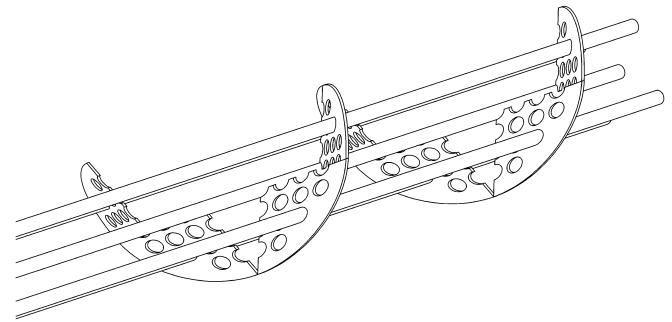


Fig. 2. Four pieces middle-overlapped helical baffle arrangement.

Table 1

Geometries of the STHXsHB in open experimental studies.

Researchers	Inner diameter of the shell/mm	Effective length/mm
Zhang et al. [12]	139.8	714
Zhang et al. [15]	110	750
Liu et al. [16]	51	195
Wang et al. [26]	207	620
Peng et al. [27]	207	620
Wang et al. [29]	210	1598
Chen et al. [33]	207	620

And both of the oil coolers are practical products. The results are beneficial for the design and practical operation of OCSB and OCHB. And reliable experimental data is also useful for numerical method validation. Finally suggestions on the performance improvement of OCHB are given.

2. Experiment system and method

The geometry parameters of the OCSB and OCHB are listed in Tables 2 and 3, respectively. The details of experiment system and experimental method can be found in Ref. [14]. The schematic of the experiment system is shown in Fig. 3. For the readers' convenience, brief introduction on the experiment system and experiment method is supplied. The conductive-320 oil is used as the shell-side heat transfer medium. The oil is driven by a pump to conduct the heat exchange process. The oil is heated by an adjustable electric heater. The volume flow rate of oil can be adjusted by the electrically operated valve. For the water cycle, the cooling water is pumped into the system from the water tank, and passes through the tube side of the heat exchanger. After that, the heated water is cooled down by the air cooling tower and returns to the water tank for re-usage. The volume flow rate of water is also

Table 2

Geometry of the OCSB.

Item	Dimensions and description	
Shell side parameters	D_o/D_i /mm	325/309
	Material	Stainless steel
Tube parameters	d_o/d_i /mm	10/8
	Effective length/mm	2385
	Number	440
	Layout pattern	30°
	Tube pitch/mm	13
Baffle parameters	Material	Stainless steel
	Tube pass	2
	Cut ratio	25%
	Thickness/mm	2.5
	Number	19
	Baffle pitch/mm	110

Table 3
Geometry of the OCHB.

Item		Dimensions and description
Shell side parameters	D_o/D_i /mm	325/309
	Material	Stainless steel
Tube parameters	d_o/d_i /mm	10/8
	Effective length/mm	2250
	Number	440
	Layout pattern	30°
	Tube pitch/mm	13
	Material	Stainless steel
	Tube pass	2
Baffle parameters	Baffle pitch/mm	195
	Helix angle	15°
	Thickness/mm	2.5
	Number	44

Table 4
The test range and accuracy of instruments.

Instruments	Range	Accuracy
Platinum resistance thermometers	−100 to 200 °C	0.15 °C
Turbo volume flow meters	8.5–60 m ³ /h	1.0%
Pressure drop transmitter	0–100 kPa	0.25%

3. Data reduction

3.1. Determination of shell side velocity and Re number

The shell side fluid mean velocity is defined by

$$u = \frac{q_s}{A_{cross}} \tag{1}$$

where A_{cross} is the cross-flow area at the shell centerline [9,36],

For the helical baffle:

$$A_{cross} = 0.5B \left[D_i - D_1 + \frac{D_1 - d_o}{t_p} (t_p - d_o) \right] \tag{2}$$

And for the segmental baffle:

$$A_{cross} = B \left[D_i - D_1 + \frac{D_1 - d_o}{t_p} (t_p - d_o) \right] \tag{3}$$

adjusted by the electrically operated valve located in the water loop. Considering that the value of oil dynamic viscosity changes with temperature significantly, the average magnitudes of inlet and outlet temperatures in shell side are kept around 35.5 °C in all test cases in order to reduce errors of physical properties calculation and obtain more accurate correlation for heat transfer and pressure drop. The oil temperature range was quite strictly controlled by adjusting the power of electrical heater for oil. The test range and accuracy of the measurements are given in Table 4.

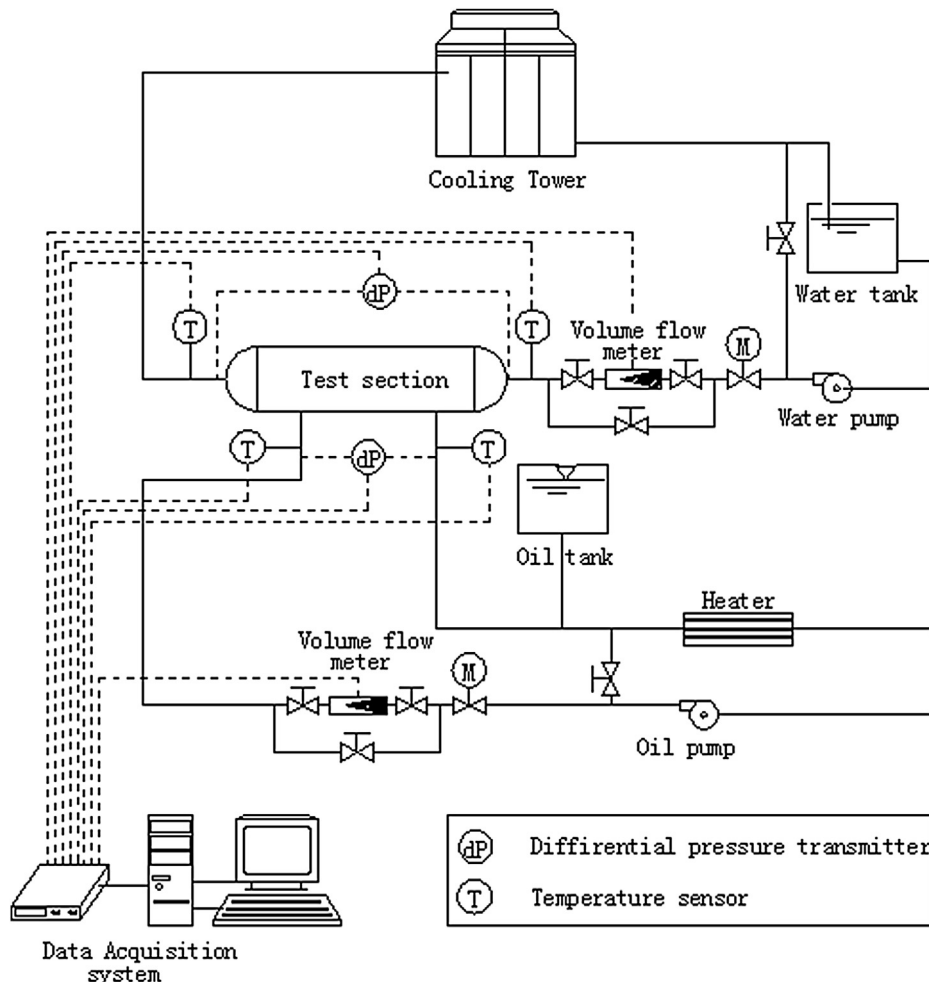


Fig. 3. Experiment system schematic.

where D_i is the inside diameter of shell, D_1 is the diameter of the tube bundle-circumscribed circle, d_o is the tube outside diameter, and t_p is the tube pitch.

For the segmental baffle and the continuous helical baffle the determination of B is quite straightforward. For the four pieces overlapped helical baffle arrangement B is determined as follows:

$$B = 2\sqrt{2}\alpha \cdot D_1 \cdot \tan \beta, \quad 0 < \alpha \leq 1 \quad (4)$$

where α is the overlapped rate of the helical baffles (see Fig. 4), e.g. for four pieces middle overlapped helical baffle arrangement $\alpha = 0.5$, and for the continuous connection arrangement $\alpha = 1.0$.

With the mean velocity at hand, the Reynolds number of shell-side fluid can be calculated:

$$Re_s = \frac{ud_o}{\nu_s} \quad (5)$$

where the subscript s refer to shell-side.

3.2. Heat transfer rate

Heat transfer rate of shell side fluid:

$$Q_s = M_s \times c_{p,s} \times (T_{s,in} - T_{s,out}) \quad (7)$$

Heat transfer rate of tube side fluid is:

$$Q_t = M_t \times c_{p,t} \times (T_{t,out} - T_{t,in}) \quad (8)$$

where M is mass flow rate, t is temperature, c_p is specific heat. The reference temperature for the fluid thermodynamic and transport properties of water and oil are the average temperature of the inlet and outlet for the test section. The subscript t refers to tube side.

Average heat transfer rate is defined as:

$$Q_{ave} = (Q_s + Q_t)/2 \quad (9)$$

Heat balance deviation in percentage is:

$$\varepsilon = \frac{|Q_s - Q_t|}{Q_{ave}} \times 100\% \quad (10)$$

During the test, the heat balance deviation should be less than 5.0% for each run.

3.3. Over-all heat transfer coefficient

The overall heat transfer coefficient, k , is defined by

$$k = \frac{Q_{ave}}{A_o \cdot \Delta T_m} \quad (11)$$

$$A_o = N_t \cdot \pi d_o l \quad (12)$$

$$\Delta t_m = \psi \frac{\Delta T_{max} - \Delta T_{min}}{\ln(\Delta T_{max}/\Delta T_{min})} \quad (13)$$

$$\Delta T_{max} = T_{s,in} - T_{t,out} \quad (14)$$

$$\Delta T_{min} = T_{s,out} - T_{t,in} \quad (15)$$

where A_o is the heat exchange area based on the outer diameter of tube. Since the test pieces are two tube passes with counter-flow

arrangement, the correct factor for the logarithmic mean temperature difference is determined by Ref.[37]

$$\psi = \frac{\sqrt{R^2 + 1} \cdot \ln\left(\frac{1 - P}{1 - PR}\right)}{(R - 1) \cdot \ln\left(\left[\frac{2 - P(R + 1 - \sqrt{R^2 + 1})}{2 - P(R + 1 + \sqrt{R^2 + 1})}\right]\right)} \quad (16)$$

$$P = \frac{T_{t,out} - T_{t,in}}{T_{s,in} - T_{t,in}} \quad (17)$$

$$R = \frac{T_{s,in} - T_{s,out}}{T_{t,out} - T_{t,in}} \quad (18)$$

3.4. Heat transfer coefficient of tube side

The average heat transfer coefficient of tube side is calculated by Gnielinski equation [38,39], shown by Equations (19)–(21), where the average value of the inlet and outlet temperature of working fluid is taken as the reference temperature. The characteristic dimension is the inner diameter of the tube.

$$Nu_t = \frac{(f_t/8)(Re - 1000)Pr_t}{1 + 12.7\sqrt{f_t/8}(Pr_t^{2/3} - 1)} \left[1 + \left(\frac{d_i}{l}\right)^{2/3}\right] c_t \quad (19)$$

$$f_t = (1.82 \lg Re - 1.64)^{-2} \quad (20)$$

$$c_t = \left(\frac{Pr_f}{Pr_w}\right)^{0.11} \quad (21)$$

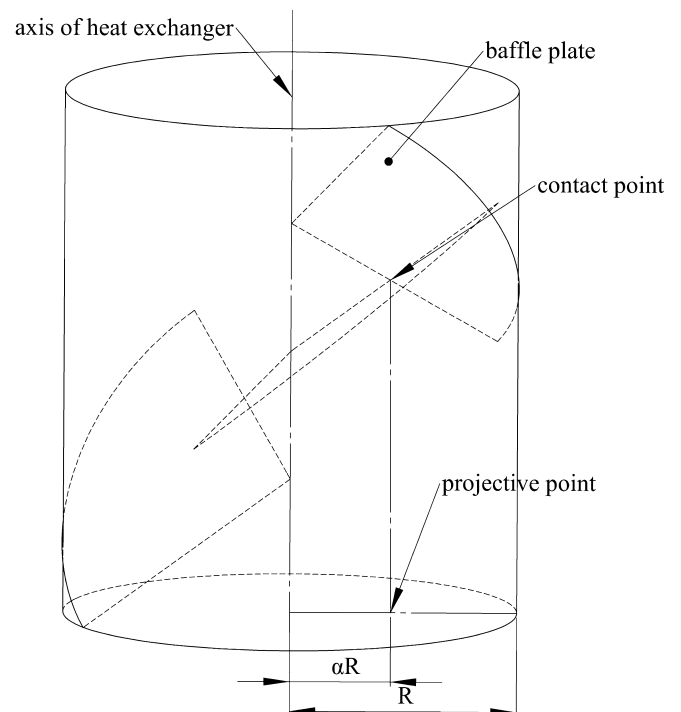


Fig. 4. Definition of overlapped rate.

3.5. Shell side heat transfer coefficient and Nu number

The average shell-side heat transfer coefficient can be obtained by the thermal resistance separation method or the Wilson plot technique with the overall heat transfer coefficient and the tube-side heat transfer coefficient [39,40]:

$$\frac{1}{k} = \frac{1}{h_t} \frac{d_o}{d_i} + \frac{d_o}{2\lambda_w} \ln \frac{d_o}{d_i} + \frac{1}{h_s} \quad (22)$$

$$Nu_s = \frac{h_s d_o}{\lambda_s} \quad (23)$$

The tube wall is made from stainless steel and its thermal conductivity is taken as constant (15.2 W/(m K)).

3.6. Data fitting

The Nu numbers obtained in the test are fitted into following correlations [41,42]:

$$Nu_s = c Re_s^m Pr_s^{1/3} \quad (24)$$

3.7. Experimental uncertainty

The values of uncertainties for the entire measurement range are given in Table 5, which are estimated by the procedure described by Kline and McClintock [43] and Moffat [44].

4. Results and discussion

4.1. Pressure drop

It can be clearly observed from Fig. 5 that the shell-side pressure drop of the OCHB is significantly lower than (47.65%–50.57%) that of the OCSB under the same flow rate. The significant increase in the shell-side pressure drop for the OCSB is obviously caused by the zigzag flow pattern, which has been indicated by many researchers [5,8,10,14].

4.2. Heat transfer

Fig. 6 shows the variation of shell-side average heat transfer coefficients along the oil volume flow rate. It can be found that, under the same oil volume flow rate, the shell-side heat transfer coefficients of the OCHB are lower than that of the OCSB. In principle, the flow in the shell side of the segmental baffle can be regarded as cross flow around the tube bank. And the flow in the shell side of the helical baffles can be regarded as heat transfer across the tube bank at specific angles. It is well-known in heat transfer theory that at the same velocity the heat transfer of cross-flow is stronger than that of inclined flow. Hence at the same flow rate, the heat transfer coefficient of the OCHB is less than that of OCSB.

The correlations between Nu and Re_s for each heat exchanger are obtained as follows with the maximum deviations shown in the

parentheses. And the graphical presentations of the fitting equations are shown in Fig. 7.

Segmental baffles:

$$Nu_s = 0.012 Re_s^{0.98} Pr_s^{1/3} \quad (-3.14\%) \quad (25)$$

Helical baffles:

$$Nu_s = 0.037 Re_s^{0.75} Pr_s^{1/3} \quad (-3.47\%) \quad (26)$$

From Figs. 5 and 6, it can be found that under the same shell-side flow rate, although shell side heat transfer coefficient of the OCHB is lower than that of the OCSB, the shell-side pressure drop of the OCHB is even much lower than that of the OCSB, which indicates that under the same shell side pressure drop, the shell-side heat transfer coefficient of the OCHB are higher than that of the OCSB.

4.3. Comprehensive performance analysis

Shell-side heat transfer coefficient per unit pressure drop at the same shell-side flow rate is adopted to investigate the comprehensive performance of the OCHB and OCSB, because that in practical application the pressure drop of the heat exchangers are usually limited, the shell-side heat transfer coefficient per unit pressure drop at the same shell-side flow rate should be a more reasonable comparison quantity [14]. Comparisons of heat transfer coefficient per unit pressure drop of each heat exchanger are given in Fig. 8. It can be found that the heat transfer coefficients per unit pressure drop of the OCHB are 51.8%–76.4% higher than that of the OCSB.

Based on the experimental results discussed above, it can be easily understood that if a new heat exchanger with helical baffle is designed to replace a heat exchanger with segmental baffles, when the new heat exchanger has equal pressure drop as the original heat exchanger, its heat transfer capacity must be larger than that of the original one; and when the new designed heat exchanger has equal heat transfer capacity as the original heat exchanger, then it can definitely save much pumping power.

4.4. Performance improvement of OCHB

In order to enhance the heat transfer performance of OCHB, it is vital to increase the shell side velocity, thus leading to the increase of shell side pressure drop, and then the OCHB will definitely get higher heat transfer coefficients than OCSB because of the higher heat transfer coefficients per unit pressure drop. For example, if the overlapped rate of OCHB in the present study is changed to be 0.5 (middle overlapped arrangement), the helix pitch will change from 197 mm to 117 mm, and the shell side velocity will increased by 68.38%. With test data at hand, the pressure drop and heat transfer coefficient can be estimated by extrapolation method. The shell side heat transfer coefficient of the OCHB will be 19.86%–36.28% higher than that of the OCSB and the pressure drop will be 13% higher than that of the OCSB at the most. It could be concluded that with proper design the OCHB can successfully replace the OCSB with reducing heat transfer area (smaller size) to save material cost. And the OCHB can also contribute to capital cost saving in pumping equipment, operation and maintenance because of lower fouling resistance. The helical baffle design offers greater flexibility in selecting the optimum helix angles and overlapped rate to maintain the desired flow velocities.

Table 5
Experiment uncertainties.

Item	Segmental baffle	Helical baffle
Pressure drop %	±(0.81–2.25)%	±(1.71–5.68)%
Heat transfer rate %	±(7.42–8.85)%	±(8.66–9.87)%
Overall heat transfer coefficient %	±(7.43–8.85)%	±(8.67–9.87)%

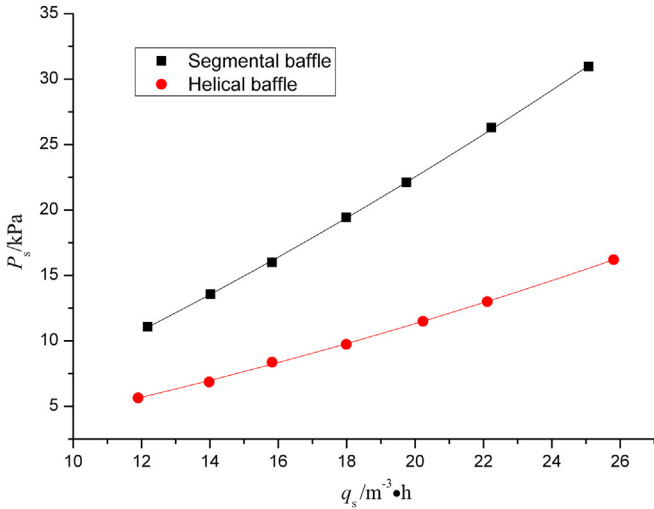


Fig. 5. Shell side pressure drop versus flow rate of shell side.

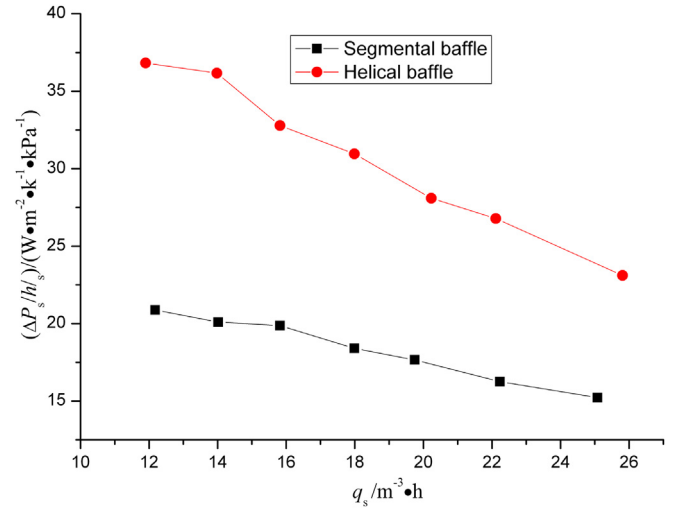


Fig. 8. Shell side heat transfer coefficient per unit pressure drop versus flow rate in shell side.

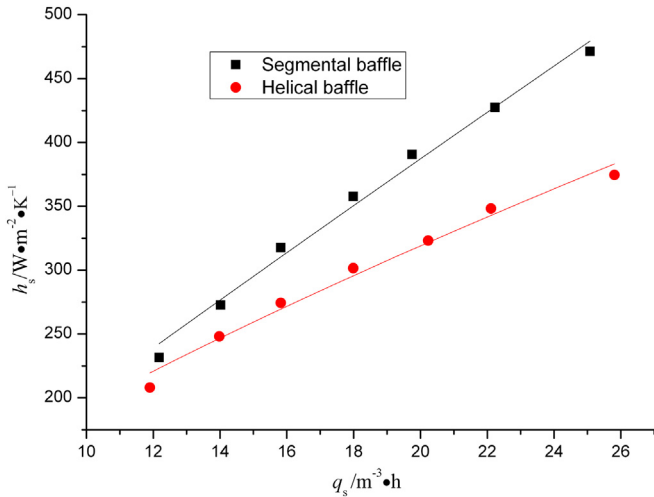


Fig. 6. Shell side heat transfer coefficient versus flow rate.

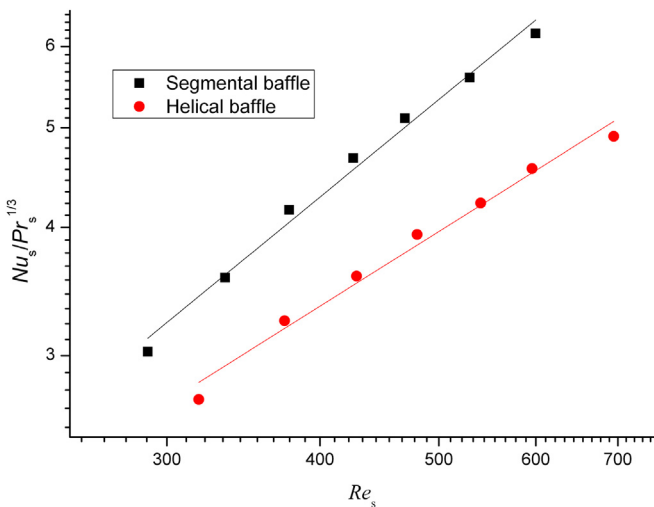


Fig. 7. Nu number versus Re number in shell side.

5. Conclusions

The flow and heat transfer characteristics of shell-and-tube oil coolers with segmental baffles and helical baffles are experimentally studied. And both of the oil coolers are practical products. The results show that:

1. For the same volume flow rate, the shell side heat transfer coefficients of the OCHB are lower than that of the OCSB, while the shell-side pressure drop of the former is far lower than that of the later;
2. The OCHB has a much higher heat transfer coefficient per unit pressure drop at the same volume flow rate;
3. In order to enhance heat transfer performance of the OCHB, one effective method is to increase the shell side velocity of the OCHB by selecting the optimum helix angles and overlapped rate in the design.

Acknowledgements

This work is supported by National Natural Science Foundation of China (No. 51206129) and National Basic Research Program of China (973 Program) (No. 2013CB228304). The test heat exchangers were supplied by Hangzhou Hangyang Heat Exchanger Equipment Co. LTD.

Notation

Latin symbols

- A_{cross} cross-flow area per baffle spacing through pass partition lanes at the shell centerline, mm^2
- A_o heat exchange area based on the outer diameter of tube, mm^2
- B baffle spacing for segmental baffles or helical pitch for helical baffles, mm
- c constant in curve fitting
- c_t thermophysical properties correction factor
- c_p specific heat, $kJ/(kg \cdot K)$
- D_i inside diameter of shell, mm
- D_o outside diameter of shell, mm
- D_1 tube bundle-circumscribed circle diameter, mm
- d_i tube inner diameter, mm

d_o	outer diameter of tube, mm
f_t	Darcy friction factor for turbulence flow inside tube
h	heat transfer coefficient, $W (m^2 K)^{-1}$
k	Overall heat transfer coefficient, $W (m^2 K)^{-1}$
l	effective length of tube, mm
m	constant in curve fitting
M	mass flux, kg/s
N	tube number
N_t	number of tube rows
Nu	Nu number
ΔP	pressure drop, kPa
Pr	Pr number
Pr_f	Pr number at the reference temperature of fluid
q	volume flow rate, $m^3 h^{-1}$
Re	Re number
S_p	the thickness of baffle, mm
ΔT_m	logarithmic mean temperature difference, K
T	temperature, K
t_p	tube pitch, mm
u	fluid velocity in the shell side, $m s^{-1}$

Greek symbols

α	overlapped ratio
β	helix angle
ε	heat balance deviation
Φ	heat exchange quantity, W
Φ_{ave}	average heat exchange quantity, W
λ	conductivity factor, $W (m K)^{-1}$
ρ	density, $kg m^{-3}$
ν	kinematics viscosity, $m^2 s^{-1}$

Subscripts

in	inlet
out	outlet
s	shell side
t	tube side
w	tube wall

References

- [1] B.I. Master, K.S. Chunangad, V. Pushpanathan, Fouling mitigation using helixchanger heat exchangers, in: Proceedings of the ECI Conference on Heat Exchanger Fouling and Cleaning: Fundamentals and Applications, May 18–22, 2003, Santa Fe, NM, pp. 317–322.
- [2] R. Mukherjee, Use double-segmental baffles in the shell-and-tube heat exchangers, Chem. Eng. Prog. 88 (1992) 47–52.
- [3] M. Saffar-Avval, E. Damangir, A general correlation for determining optimum baffle spacing for all types of shell and tube exchangers, Int. J. Heat Mass. Transfer 38 (1995) 2501–2506.
- [4] H.D. Li, V. Kottke, Effect of baffle spacing on pressure drop and local heat transfer in shell-and-tube heat exchangers for staggered tube arrangement, Int. J. Heat Mass. Transfer 41 (1998) 1303–1311.
- [5] P. Sthliik, V.V. Wadekar, Different strategies to improve industrial heat exchange, Heat Transfer Eng. 23 (2002) 36–48.
- [6] K.J. Bell, Heat exchanger design for the process industries, ASME J. Heat Transfer 126 (2004) 877–885.
- [7] B.K. Soltan, M. Saffar-Avval, E. Damangir, Minimization of capital and operating costs of shell and tube condensers using optimum baffle spacing, Appl. Therm. Eng. 24 (2004) 2801–2810.
- [8] J. Lutchka, J. Nemcansky, Performance improvement of tubular heat exchangers by helical baffles, Trans. ChemE 68 (1990) 263–270.
- [9] P. Stehlik, J. Nemcansky, D. Kral, Comparison of correction factors for shell-and-tube heat exchangers with segmental or helical baffles, Heat Transfer Eng. 15 (1994) 55–65.
- [10] D. Kral, P. Stehlik, H.J. Van Der Ploeg, I.M. Bashir, Helical baffles in shell-and-tube heat exchangers, part one: experimental verification, Heat Transfer Eng. 17 (1996) 93–101.
- [11] S.L. Wang, Hydrodynamic studies on heat exchangers with helical baffles, Heat Transfer Eng. 23 (2002) 43–49.
- [12] Z.G. Zhang, T. Xu, X.M. Fang, Experimental study on heat transfer enhancement of a helically baffled heat exchanger combined with three-dimensional finned tubes, Appl. Therm. Eng. 24 (2004) 2293–2300.
- [13] Y.G. Lei, Y.L. He, P. Chu, R. Li, Design and optimization of heat exchangers with helical baffles, Chem. Eng. Sci. 63 (2008) 4386–4395.
- [14] J.F. Zhang, B. Li, W.J. Huang, Y.G. Lei, Y.L. He, W.Q. Tao, Experimental performance comparison of shell side heat transfer for shell-and-tube heat exchangers with middle-overlapped helical baffles and segmental baffles, Chem. Eng. Sci. 64 (2009) 1643–1653.
- [15] Z.G. Zhang, Q.X. Li, T. Xu, X.M. Fang, X.N. Gao, Condensation heat transfer characteristics of zeotropic refrigerant mixture R407C on single, three-row petal-shaped finned tubes and helically baffled condenser, Appl. Therm. Eng. 39 (2012) 63–69.
- [16] L. Liu, X. Ling, H. Peng, Analysis on flow and heat transfer characteristics of EGR helical baffled cooler with spiral corrugated tubes, Exp. Therm. Fluid Sci. 44 (2013) 275–284.
- [17] B. Deng, Experimental and Numerical Study of Flow and Heat Transfer in the Shell Side of Heat Exchangers. Ph.D. thesis, Xi'an Jiaotong University, Xi'an, China, 2003.
- [18] M.J. Andrews, B.I. Master, 3-D modeling of the ABB lummus heat transfer helixchanger using CFD, in: International Conference on Compact Heat Exchangers, Banff, Canada, 1999.
- [19] M.J. Andrews, B.I. Master, Three-dimensional modeling of a helixchanger® heat exchanger using CFD, Heat Transfer Eng. 26 (2005) 22–31.
- [20] R.J. Shen, X. Feng, X.D. Gao, Mathematical model and numerical simulation of helical baffles heat exchanger, J. Enhanc. Heat Transfer 11 (2004) 461–466.
- [21] Y.G. Lei, Y.L. He, R. Li, Y.F. Gao, Effects of baffle inclination angle on flow and heat transfer of a heat exchanger with helical baffles, Chem. Eng. Process. Process Intensifi. 47 (2008) 2336–2345.
- [22] M.R. Jafari Nasr, A. Shafeghat, Fluid flow analysis and extension of rapid design algorithm for helical baffle heat exchangers, Appl. Therm. Eng. 28 (2008) 1324–1332.
- [23] J.F. Zhang, Y.L. He, W.Q. Tao, 3D numerical simulation on shell-and-tube heat exchangers with middle-overlapped helical baffles and continuous baffles—part I: numerical model and results of whole heat exchanger with middle-overlapped helical baffles, Int. J. Heat Mass. Transfer 52 (2009) 5371–5380.
- [24] J.F. Zhang, Y. L.He, W.Q. Tao, 3D numerical simulation on shell-and-tube heat exchangers with middle-overlapped helical baffles and continuous baffles—part II: simulation results of periodic model and comparison between continuous and noncontinuous helical baffles, Int. J. Heat Mass. Transfer 52 (2009) 5381–5389.
- [25] F.N. Taher, S.Z. Movassag, K. Razmi, R.T. Azar, Baffle space impact on the performance of helical baffle shell and tube heat exchangers, Appl. Therm. Eng. 44 (2012) 143–149.
- [26] Q.W. Wang, G.N. Xie, B.T. Peng, L.Q. Luo, Experimental study and genetic-algorithm-based correlation on shell-side heat transfer and flow performance of three different types of shell-and-tube heat exchangers, ASME J. Heat Transfer 129 (9) (2007) 1277–1285.
- [27] B.T. Peng, Q.W. Wang, C. Zhang, G.N. Xie, L.Q. Luo, Q.Y. Chen, M. Zeng, An experimental study of shell-and-tube heat exchangers with continuous helical baffles, ASME J. Heat Transfer 129 (10) (2007) 1425–1431.
- [28] Q.W. Wang, Q.Y. Chen, G.D. Chen, Numerical investigation on combined multiple shell-pass shell-and-tube heat exchangers with continuous helical baffles, Int. J. Heat Mass. Transfer 52 (2009) 1214–1222.
- [29] Q.W. Wang, G.D. Chen, J. Xu, Y.P. Ji, Second-law thermodynamic comparison and maximal velocity ratio design of shell-and-tube heat exchangers with continuous helical baffles, ASME J. Heat Transfer 132 (10) (2010) 101801.
- [30] Q.W. Wang, G.D. Chen, Q.Y. Chen, M. Zeng, Review of improvements on shell-and-tube heat exchangers with helical baffles, Heat Transfer Eng. 31 (2010) 836–853.
- [31] Q.W. Wang, G.D. Chen, M. Zeng, Q.Y. Chen, B.T. Peng, D.J. Zhang, L.Q. Luo, Shell-side heat transfer enhancement for shell-and-tube heat exchangers by helical baffles, Chem. Eng. Trans. 21 (2010) 217–222.
- [32] G.D. Chen, M. Zeng, Q.W. Wang, S.Z. Qi, Numerical studies on combined parallel multiple shell-pass shell-and-tube heat exchangers with continuous helical baffles, Chem. Eng. Trans. 21 (2010) 229–234.
- [33] G.D. Chen, M. Zeng, Q.W. Wang, Experimental and numerical studies on shell-side performance of three different shell-and-tube heat exchangers with helical baffles, J. Enhanc. Heat Transfer 18 (5) (2011) 449–463.
- [34] S. Ji, W.J. Du, P. Wang, L. Cheng, Numerical investigation on double shell-pass shell-and-tube heat exchanger with continuous helical baffles, J. Thermodyn. (2011). Article ID 839468, 1–7.
- [35] Y.P. Chen, Y.J. Sheng, C. Dong, J.F. Wu, Numerical simulation on flow field in circumferential overlap trisection helical baffle heat exchanger, Appl. Therm. Eng. 50 (1) (2013) 1035–1043.
- [36] U. Schlünder Ernst (Ed.), Heat Exchanger Design Handbook, vol. 3, Hemisphere Publishing Corporation, 1983.
- [37] G.F. Hewitt, G.L. Shires, T.R. Boll, Process Heat Transfer, CRC Press, 1994.
- [38] V. Gnielinski, New equations for heat and mass transfer in turbulent pipe and channel flows, Int. Chem. Eng. 16 (1976) 359–368.
- [39] S.M. Yang, W.Q. Tao, Heat Transfer, fourth ed., Higher Education Press, Beijing, 2006.

- [40] J.W. Rose, Heat-transfer coefficient, Wilson plots and accuracy of thermal measurements, *Exp. Therm. Fluid Sci.* 28 (2004) 77–86.
- [41] S.W. Churchill, M. Bernstein, A correlating equation for forced convection from gases and liquids to a circular cylinder in cross flow, *ASME J. Heat Transfer* 99 (1977) 300–306.
- [42] Y.A. Cengel, *Heat Transfer, a Practical Approach*, WCB McGraw-Hill, Boston, 1998.
- [43] S.J. Kline, F.A. McClintock, Describing uncertainties in single-sample experiments, *Mech. Eng.* 75 (1953) 3–8.
- [44] R.J. Moffat, Describing the uncertainties in experimental results, *Exp. Therm. Fluid Sci.* 1 (1988) 3–17.